

# PART IV

## Orographic Mesoscale Phenomena

# 11

## Thermally Forced Winds in Mountainous Terrain

Part IV treats orographic mesoscale phenomena. In this chapter we consider the diurnally varying winds generated by the heating and cooling of sloped terrain, or by the differences in the diurnal temperature ranges within valleys compared with surrounding plains. Sometimes generically referred to as *mountain-valley wind systems* or just *mountain winds*, these thermally forced circulations do not require the presence of ambient winds and large-scale pressure gradients. Mesoscale phenomena that arise from interactions between ambient winds and terrain, such as gravity waves, severe downslope winds, trapped cold-air surges, gap winds, and wake vortices, are the foci of Chapters 12 and 13.

Most of the early studies on mountain-valley wind systems originated in Germany and Austria, and investigated the effects of the complex Alpine topography. Mountain-valley wind systems are characterized by a reversal of wind direction twice each day and develop over a wide range of scales. The circulations tend to be most significant when the large-scale wind is weak and the diurnal cycle has its greatest amplitude, that is, when nights are clear and days are sunny. The main components of the mountain-valley wind system are *slope winds*, which are upslope during the day and downslope at night, and *valley winds*, which are upvalley during the day and downvalley at night.<sup>1</sup> Slope winds and valley winds are discussed separately in greater detail in the following sections.

<sup>1</sup> Sometimes the term *valley winds* refers to upvalley winds, and sometimes the term *mountain winds* refers to downvalley winds.

### 11.1 Slope winds

Slope winds are driven by the horizontal buoyancy gradients that arise between air in contact with a heated or cooled sloped surface and air at the same altitude that is far enough away from the surface that it is relatively unaffected by the heating and cooling of the surface. The daytime heating of a mountain slope induces upslope or *anabatic* winds, and the night-time radiative cooling of a mountain slope generates downslope or *katabatic* winds. The momentum equations in a coordinate system oriented along and perpendicular to a slope of constant inclination angle  $\alpha$  are<sup>2</sup>

$$\frac{\partial u}{\partial t} + u \frac{\partial u}{\partial s} + w \frac{\partial u}{\partial n} = -\frac{1}{\rho} \frac{\partial p'}{\partial s} + B \sin \alpha - \frac{\partial \overline{u'w'}}{\partial n} \quad (11.1)$$

$$\frac{\partial w}{\partial t} + u \frac{\partial w}{\partial s} + w \frac{\partial w}{\partial n} = -\frac{1}{\rho} \frac{\partial p'}{\partial n} + B \cos \alpha \approx 0, \quad (11.2)$$

where  $s$  and  $n$  are the upslope and slope-normal (i.e., perpendicular to the mountainside) directions, respectively,  $u$  and  $w$  are the upslope and slope-normal wind components, respectively,  $B$  is buoyancy,  $p'$  is the perturbation pressure, and  $\partial \overline{u'w'}/\partial n$  is the turbulent momentum flux divergence (turbulent friction). The other turbulent momentum fluxes in (11.1) have been neglected, as have all of the turbulent fluxes in (11.2). The Coriolis force also has been neglected. Note that the rhs of (11.2) is approximately zero if the slope flow is in hydrostatic balance normal to the slope (sometimes called *quasi-hydrostatic* balance).

<sup>2</sup> See Mahrt (1982) and Haiden (2003).

The driving force for an upslope (downslope) wind in (11.1) is the buoyancy force  $B$ , which is generated by warming (cooling) the layer of air adjacent to the slope. Alternatively, the essence of slope winds can be explained using the horizontal vorticity equation (2.90), where the heating and cooling of a sloped surface leads to horizontal buoyancy gradients and baroclinic vorticity generation. The baroclinically generated vorticity field implies upslope (downslope) winds adjacent to a heated (cooled) slope (Figures 11.1 and 11.2).

Regarding the perturbation pressure field ( $p' = p'_h + p'_{nh}$ , where  $p'_h$  is the hydrostatic pressure perturbation and  $p'_{nh}$  is the nonhydrostatic pressure perturbation; recall Section 2.5.4), for gentle slopes (i.e., small  $\alpha$ )  $p'$  is dominated by  $p'_h$ . Thus, the magnitude of  $p'$  largely depends on the magnitude and depth of the temperature perturbation associated with the slope wind. In the case of a downslope wind, the depth of the relatively cool slope flow layer typically increases with decreasing elevation; thus,  $p' (>0)$  increases in the downslope direction and the downward acceleration driven by the buoyancy force is opposed by an adverse (directed opposite the wind velocity, i.e., upslope in this case) pressure gradient force ( $\partial p'/\partial s < 0$ ). In the case of a relatively warm upslope wind, which typically deepens in the upslope direction,  $p' (< 0)$  decreases in the upslope direction and the upward acceleration driven by the buoyancy force is augmented by an upslope-directed pressure gradient force ( $\partial p'/\partial s < 0$ ) (Figure 11.3). Thus, daytime anabatic winds tend to be stronger than nighttime katabatic winds. If the terrain is steeply sloped, then a significant part of the pressure perturbation may be from the nonhydrostatic part; in these situations, both upslope and downslope winds may experience an adverse pressure gradient force that opposes the acceleration due to buoyancy.

Thermally driven upslope winds usually attain their maximum a few hours after sunrise, when the temperature contrast between the sunlit slopes and the valley atmosphere is largest. Peak speeds of  $1\text{--}5\text{ m s}^{-1}$  at a height of  $10\text{--}20\text{ m}$  above the surface are typical. Thermally driven downslope winds tend to be a maximum near sunset when slopes are first shaded. Peak speeds are usually  $1\text{--}4\text{ m s}^{-1}$  and at a height of  $1\text{--}3\text{ m}$ . Both upslope and downslope winds are characterized by a significant degree of intermittency.

Although the depth of slope winds varies with elevation and time of day/night, the depth of upslope (downslope) flows ranges from  $50$  to  $150\text{ m}$  ( $10\text{--}40\text{ m}$ ) on average. The depth of upslope winds tends to increase with increasing elevation, as mentioned above, as well as time of day, with the latter result attributable to the effects of decreasing static stability. Conversely, the depth of downslope winds increases with decreasing elevation (see, e.g., Figure 11.2), with a reasonable estimate of the depth of the downslope flow at any particular location along the slope being roughly 5% of the drop in elevation from the crest of the ridge (e.g.,  $100\text{ m}$  below the crest, one might expect a  $5\text{ m}$  deep downslope flow).<sup>3</sup> Downslope winds also tend to decrease in depth as the night progresses as a result of increasing static stability.

The evolution of isentropic surfaces and the low-level wind field from the pre-dawn to afternoon hours in the vicinity of a mountain with an extended region of sloped terrain, similar to the terrain of the Front Range of the Rocky Mountains and the High Plains that extend to the east, is shown in Figure 11.4. An ambient westerly wind also is present. In the early morning hours, upslope flow develops within the developing mixed layer east of the highest terrain (Figure 11.4b). The mixing of westerly

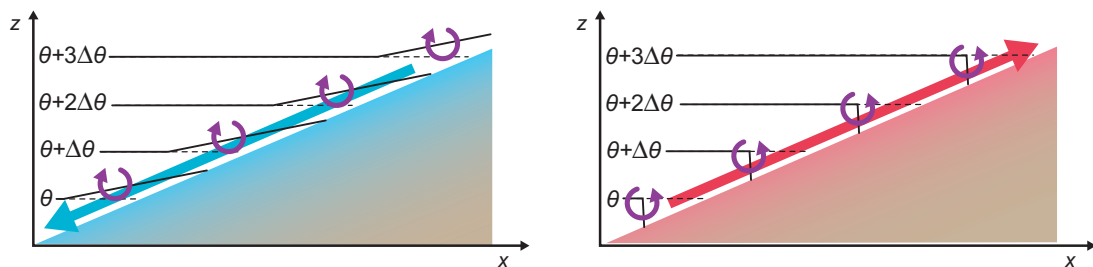


**Figure 11.1** Illustration of the generation of (left) downslope and (right) upslope winds by the cooling and heating of sloped terrain, respectively. The thick solid black contours are isentropes that have been modified by surface cooling and heating, respectively. The dashed black lines are unmodified isentropes. The purple arrows indicate the sense of the horizontal vorticity production by the horizontal buoyancy gradient. The broad blue and red arrows indicate the sense of downslope and upslope flow along the surface, respectively, implied by the baroclinic horizontal vorticity generation.

<sup>3</sup> See Whiteman (2000).

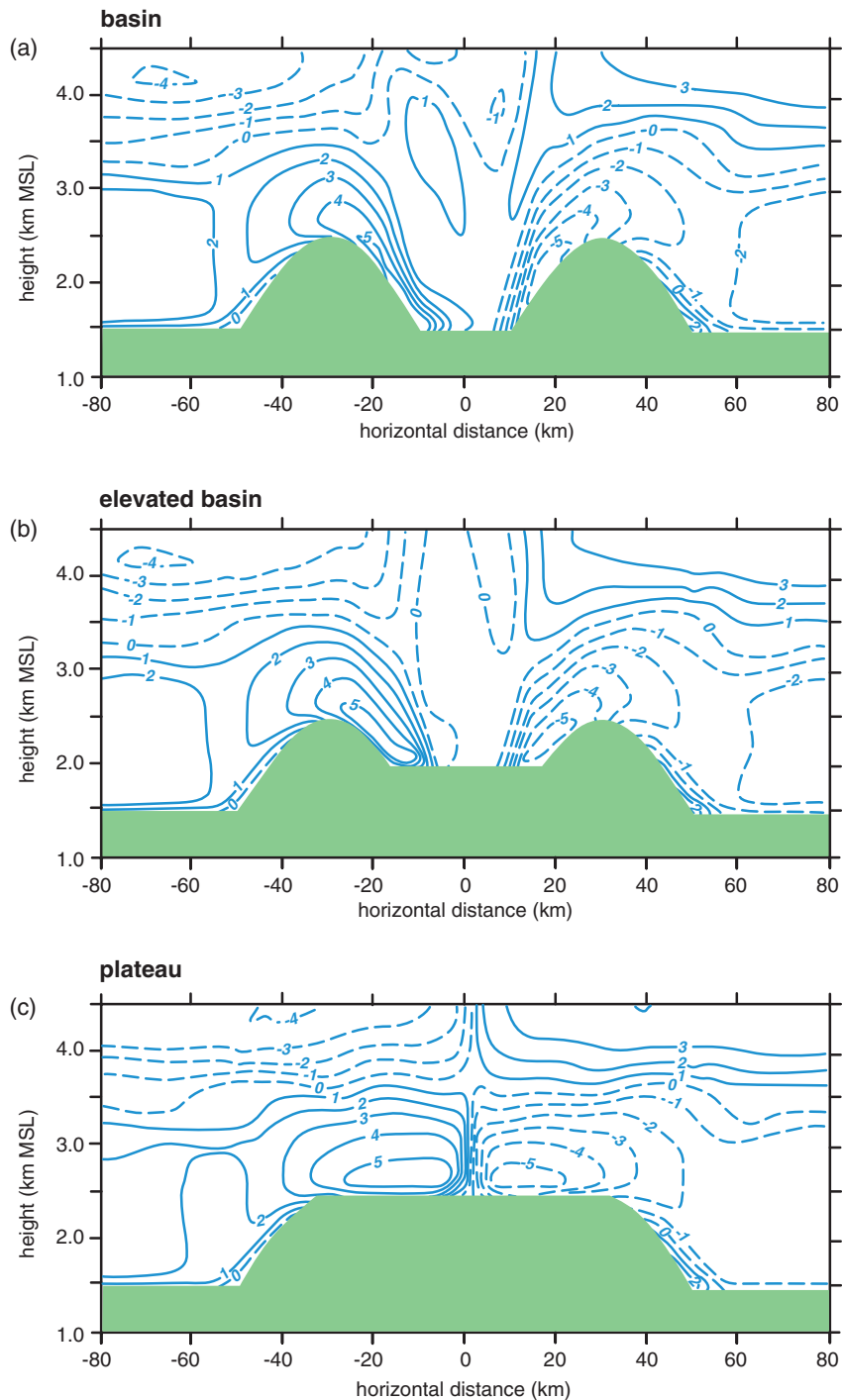


**Figure 11.2** The early evening (2000 LST) zonal wind component ( $\text{m s}^{-1}$ ) in a suite of idealized, two-dimensional numerical simulations involving diurnally varying radiative forcing, simple topography, and no ambient wind. In addition to obvious downslope winds, there are larger-scale winds that have also been thermally forced by the valley wind generation mechanism. (Adapted from de Wekker *et al.* [1998].)

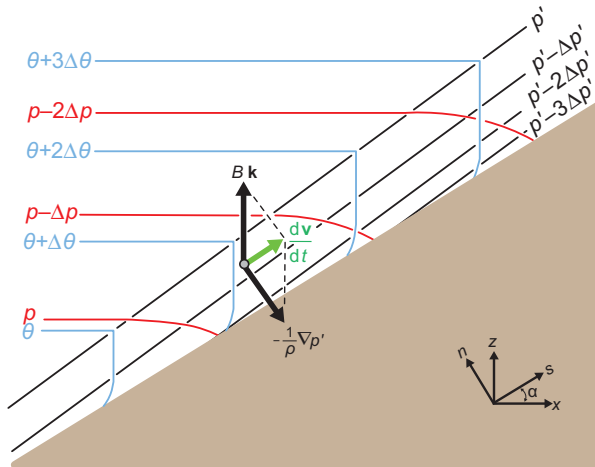


**Figure 11.3** Force diagram in the case of a daytime, thermally driven upslope flow in which the depth of the temperature perturbation increases in the upslope direction. Isentropes are blue, perturbation pressure contours are black, and full pressure contours are red. The perturbation pressure gradient gives a small positive contribution to upslope acceleration in this case. Perpendicular to the slope, the flow is quasi-hydrostatically balanced. In the special case of along-slope thermal homogeneity, the perturbation pressure contours would be parallel to the slope and the perturbation pressure gradient would be exactly perpendicular to the terrain. (Adapted from Haiden [2003].)

momentum from aloft into the developing mixed layer is inhibited by the remnant stable layer that caps the mixed layer. The depth of the mixed layer having upslope winds grows in time (Figure 11.4c). It is also apparent from Figure 11.4 (as evidenced by the closed  $\theta_1$  contour atop the mountain in Figs. 11.4b,c) why the first cumulus clouds of the day (and showers and thunderstorms, if the atmosphere is sufficiently unstable) tend to be found over mountain tops. In the presence of an ambient wind, as in the case depicted in Figure 11.4, the plume of greatest buoyancy is shifted downwind.

A region of horizontal convergence is present in the wind field near the upslope side of the maximum horizontal potential temperature (and buoyancy) gradient, and the convergence maximum shifts downslope as the day progresses. Convective clouds, including thunderstorms, also can be initiated within this convergence maximum on occasion, and convection that develops over the mountain summit often is invigorated if and when it reaches this convergence zone and the enhanced moisture to its east (this convection can develop into large convective

systems that persist well into the night-time hours).<sup>4</sup> By afternoon, at least on relatively quiescent days on which convective storms do not develop, the inversion layer is completely eroded, which allows westerly winds aloft to be mixed downward to the surface on the eastern plain. The downward mixing of westerly momentum destroys the low-level upslope flow (Figure 11.4d). As one might expect, the duration of the low-level upslope flow is lengthened (shortened) as the westerly winds aloft decrease (increase). Westerly, downslope winds continue after sunset, although these winds are a result of slope wind dynamics rather than the downward mixing of westerly momentum from aloft (Figure 11.4a).

## 11.2 Valley winds

Valley winds, also sometimes referred to as *valley breezes*, blow parallel to the longitudinal axis of a valley and arise from temperature differences that form within a valley or between a valley and a nearby plain, assuming that the valley eventually widens to a degree where it can be considered a plain. Winds blow upvalley (i.e., toward the direction of the mountains from the direction of the plains) during the day and downvalley (i.e., from the direction of the mountains toward the direction of the plains) at night (Figure 11.5), although the valley floor need not be sloped in order for valley winds to arise. The driving mechanism for valley winds is a difference in the amplitude of the diurnal temperature cycle along the axis of the valley, or between the valley, which typically has sloped sidewalls, and the surrounding plains (Figures 11.6 and 11.7). During the day, the air in the interior of the valley warms more than an equivalent vertical column of air over the adjacent plains, leading to a hydrostatically produced horizontal pressure gradient force directed from the plains toward the valley; thus, air flows upvalley (Figure 11.8). At night, the atmosphere in the valley interior cools more than the atmosphere over the plains, leading to a reversal of the horizontal pressure gradient and a downvalley flow (Figure 11.8). The combined airflow of nocturnal downvalley and downslope winds is sometimes referred to as a *drainage wind*.

Upvalley winds typically begin in the morning within a few hours after sunrise and persist until shortly after sunset, after which time they are replaced by downvalley winds. The downvalley winds, in turn, persist until being replaced by upvalley winds the next morning. Peak speeds attained by up- and downvalley winds can reach  $5\text{--}10\text{ m s}^{-1}$ . Mature

<sup>4</sup> The interaction of this slope-flow-induced convergence zone with mountain-induced gravity waves can also contribute significantly to the development of the convective systems. See Tripoli and Cotton (1989a, b).

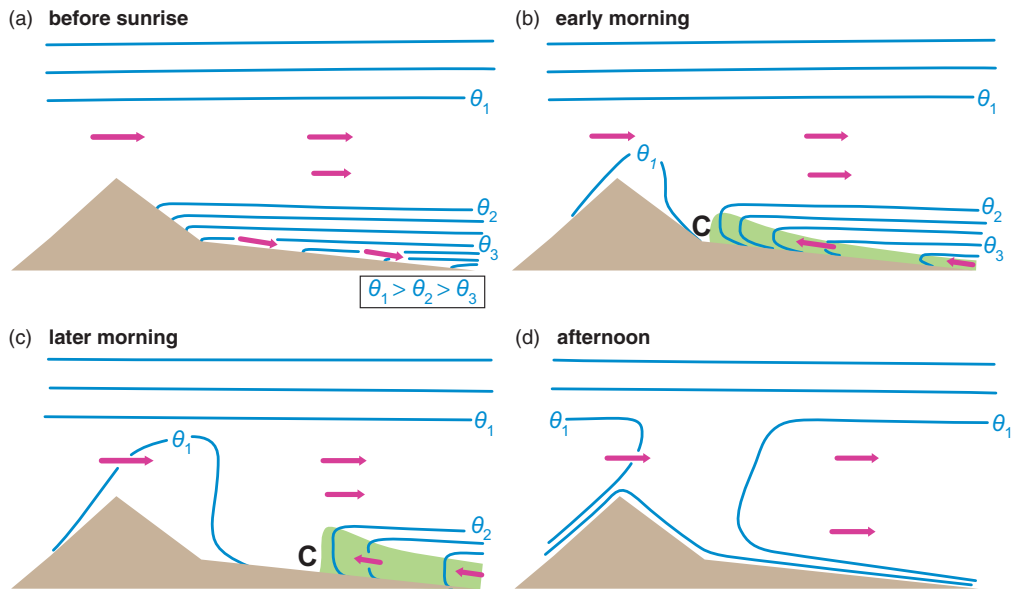


**Figure 11.4** Evolution of potential temperature and winds from (a) before sunrise to (b) early morning to (c) late morning to (d) afternoon as a result of the development of a thermally forced anabatic wind (the previous night's katabatic wind is evident in [a]). An ambient wind also is present, blowing from left to right. The shaded region indicates a shallow mixed layer that contains the upslope flow, and the C at the upwind edge indicates the convergence zone. (Adapted from Banta [1990].)

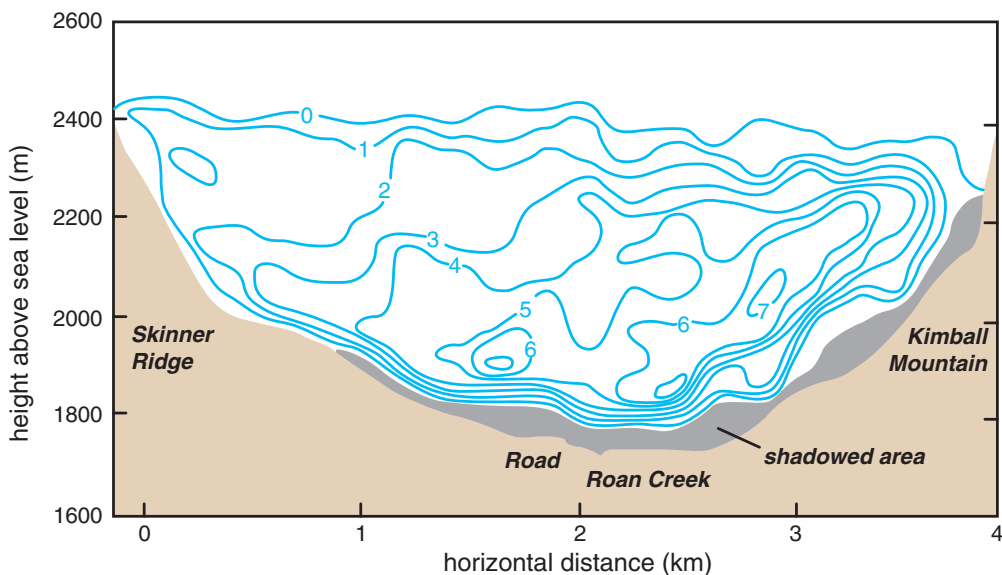


**Figure 11.5** Vertical cross-section of downvalley nocturnal drainage winds as viewed by a Doppler lidar. The isotachs indicate wind speeds out of the page ( $\text{m s}^{-1}$ ). (Adapted from Neff [1990].)

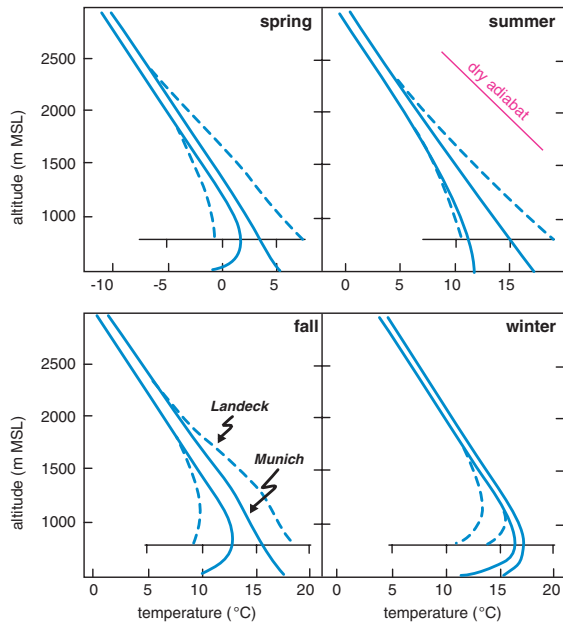


**Figure 11.6** Schematic vertical temperature profiles for a valley location (dashed lines, Landeck, Germany, at 821 m MSL in the Inn Valley) and for a location on the adjacent plain (solid lines, Munich, Germany, at 529 m MSL) at 0600 and 1500 UTC for spring, summer, fall, and winter. (Adapted from Whiteman [1990], whose figure was adapted from Nickus and Vergeiner [1984].)

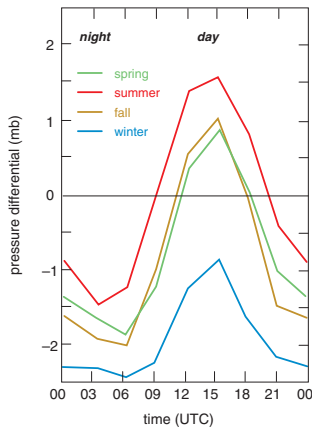


**Figure 11.7** Daily evolution of the horizontal pressure differential at 550 m MSL between a location on the plains (Munich, Germany) and a deep valley station (Innsbruck, Austria) on sunny days. (Adapted from Whiteman [1990], whose figure was adapted from Nickus and Vergeiner [1984].)

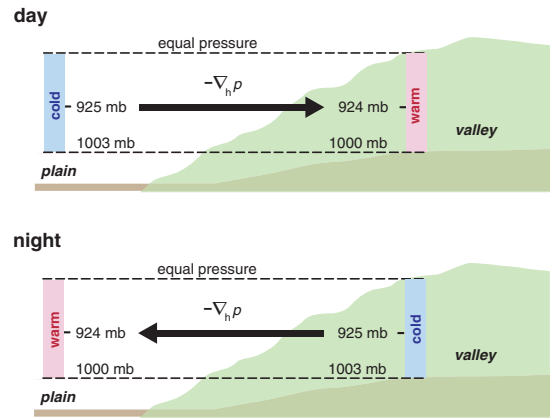


**Figure 11.8** Illustration of the origin of the horizontal pressure gradient that drives valley winds. (Adapted from Whiteman [1990], whose figure was adapted from a paper by Hawkes [1947].)

up- and downvalley flows tend to span the depth of the valley. On rare occasions the valley flows are shallower and overrun by a significant return flow called an *antiwind*. Such return flows are usually not observed directly because they tend to lie above the crests of the surrounding terrain. When the return flow occurs at such heights, it is usually too weak to detect because it is not confined to a channel like the lower branch of the circulation.

As indicated above, the primary forcing for valley winds is the horizontal pressure gradient that ultimately results from a more pronounced diurnal cycle within the valley compared with the surrounding plains. The differences in the diurnal temperature cycle are most often explained by way of the first law of thermodynamics, which, in the case of  $dp/dt = 0$ , can be written as

$$Q = C_p \frac{dT}{dt} = \rho c_p V \frac{dT}{dt}, \quad (11.3)$$

where  $Q$  is the heating rate [ $\text{J K}^{-1}$ ]; this ultimately results from the sensible heat flux, which results from an imbalance between the net radiation incident at the surface and the latent and ground heat fluxes via (4.56),  $C_p$  is the heat capacity at constant pressure,  $c_p$  is the specific heat at constant pressure,  $\rho$  is the air density,  $V$  is the volume of air, and  $dT/dt$  is the rate of temperature change. From (11.3) it is apparent that the same solar radiation flux through equal areas topping a valley and a plain results in greater warming of the smaller volume of valley air. Similarly, a smaller valley air volume will cool more at night than the surrounding plain. Thus, valleys have amplified diurnal temperature cycles.



The amplification of the diurnal temperature cycle is often quantified in terms of the *topographic amplification factor* (TAF), where

$$\text{TAF} = \frac{\left[ \frac{A_{xy}(h)}{V_{\text{valley}}} \right]}{\left[ \frac{A_{xy}(h)}{V_{\text{plain}}} \right]} = \frac{V_{\text{plain}}}{V_{\text{valley}}}, \quad (11.4)$$

where  $A_{xy}(h)$  is the horizontal area through which solar radiation enters the tops of the volumes at height  $z = h$  above the valley floor or plain, and  $V_{\text{valley}}$  and  $V_{\text{plain}}$  are the underlying volumes of the valley and plain, respectively. Note that  $V_{\text{plain}} = hA_{xy}(h)$ .

For a simple, unit-thickness, vertical cross-section through a valley, the TAF can be defined as

$$\text{TAF} = \frac{\left[ \frac{W}{A_{xz\text{valley}}} \right]}{\left[ \frac{W}{A_{xz\text{plain}}} \right]} = \frac{A_{xz\text{plain}}}{A_{xz\text{valley}}}, \quad (11.5)$$

where  $W$  is the width at the top of the cross-section, and  $A_{yz\text{valley}}$  and  $A_{yz\text{plain}}$  are the areas of the vertical cross-sections taken in the valley and adjacent plain, respectively. The numerator and denominator of (11.5) are the area-to-volume ratios for the valley and plain, respectively. In summary, the TAF is just a ratio, computed solely from the topography, of the amplitude of the diurnal temperature cycle in a valley compared with that at the same altitude over the adjacent plain (Figure 11.9).

Although the amplified diurnal temperature cycle within valleys has been identified as the primary driving force for valley winds, other effects have also been shown to contribute to valley winds, such as along-valley elevation changes (which produce upslope and downslope accelerations as discussed in Section 11.1), along-valley variations in the surface energy budget, and vertical motions associated with slope and valley wind circulations. With respect to along-valley variations in the surface energy budget, it is not difficult to imagine that albedo could vary in the along-valley direction if there is a glacier at the head of a valley and a forest at the base of the valley, or that soil moisture and thus the sensible heat flux could vary longitudinally within a valley (it conceivably could be drier near the higher-altitude head of the valley than at the lower-altitude base). Regarding the effect of vertical motions, the compensating subsidence within a valley occurring during the day as a result of upslope winds along valley sidewalls (i.e., the *cross-valley circulation*) has been found to enhance to the relative pressure minimum within the valley that drives the upvalley flow.

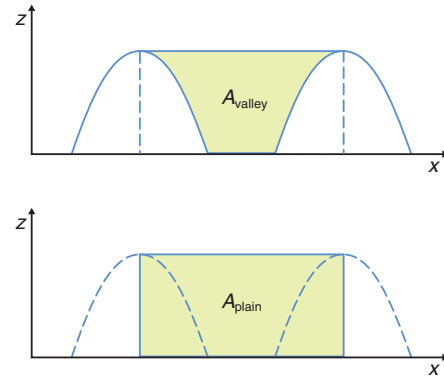


**Figure 11.9** Illustration of the topographic amplification factor concept. For this idealized valley topography, the topographic amplification factor is simply the ratio of the areas of the shaded cross-sections over the plains ( $A_{\text{plain}}$ ) and the valley ( $A_{\text{valley}}$ ). (Adapted from de Wekker *et al.* [1998].)

Similarly, the convergence of nocturnal downslope winds in a valley is associated with rising motion in the valley interior (above the surface), and the resultant adiabatic cooling has been shown to contribute to the relative pressure excess in the valley that drives the downvalley flow. In summary, even if the sidewalls of a valley were vertical, the slope winds and compensating vertical motions would still be capable of generating temperature and (hydrostatic) pressure perturbations, horizontal pressure gradients, and valley winds.

Although slope and valley winds have been treated somewhat separately above, together they produce an intrinsically three-dimensional mountain-valley wind system. Slope and valley winds can influence each other, as touched upon above in the discussion of how compensating vertical motions in the cross-valley plane can contribute to valley winds. Figure 11.10 depicts the basic characteristics of slope and valley winds in a typical diurnal cycle; this figure is reproduced in a number of reviews on slope and valley winds. The superpositioning of slope and valley winds leads to a clockwise (counterclockwise) turning of the wind in time on the left (right) side of a valley if looking upvalley (Figure 11.11).

One final issue that has been ignored up to this point is the fact that opposing valley sidewalls are unavoidably heated unequally during much of the day (e.g., eastward-facing slopes are warmer than westward-facing slopes in the morning).<sup>5</sup> The *cross-valley winds* that result from

<sup>5</sup> The surface energy budget at any particular location in an actual valley depends on the fraction of the sky visible in the viewing hemisphere, called the *sky view factor*. The distribution of sky view factors leads to complicated spatial variations in downward longwave and diffuse solar radiation that are outside the scope of this book.



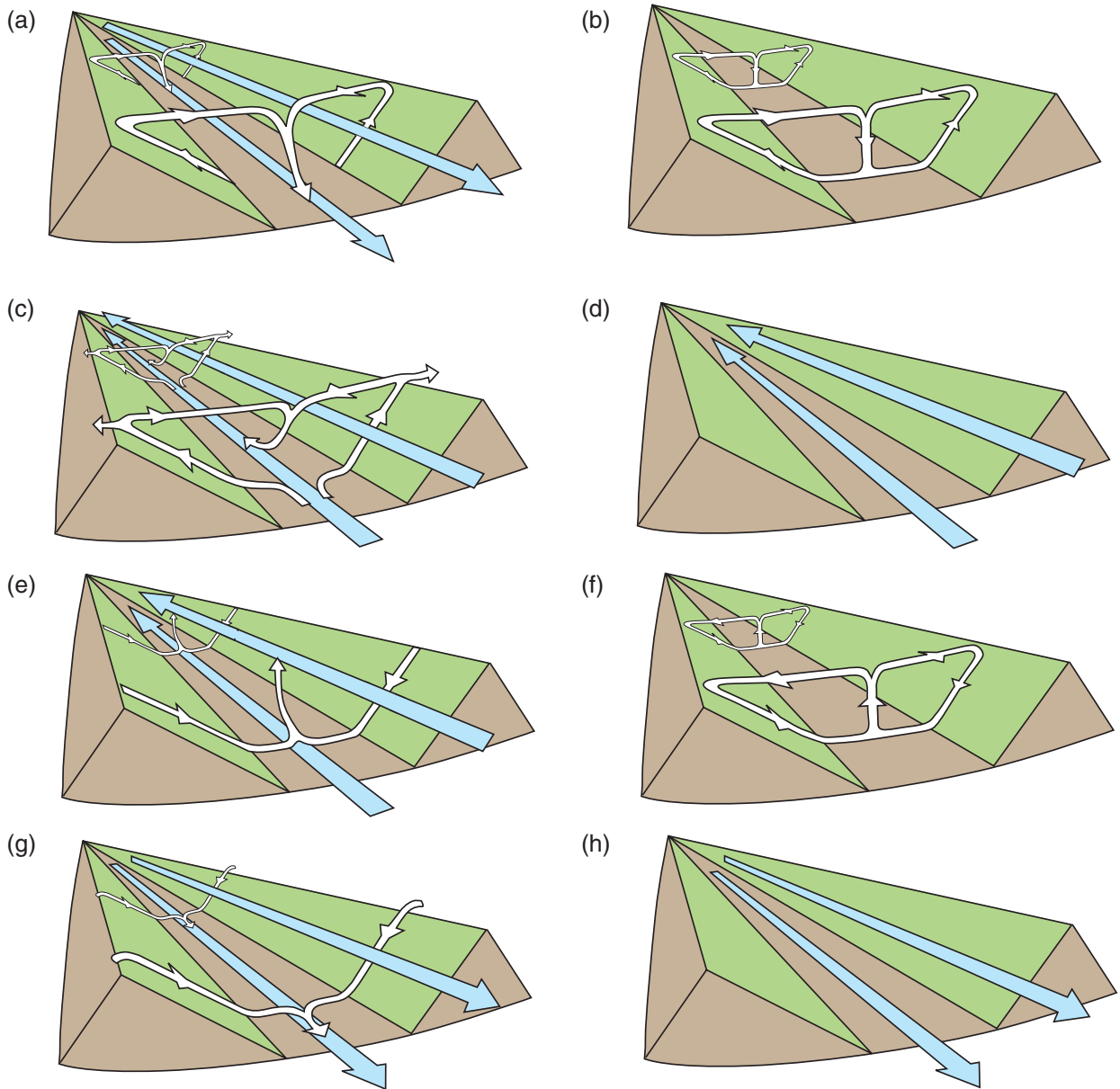


**Figure 11.10** Diurnal cycle of valley and slope winds (after Defant [1951]). (a) Sunrise: onset of upslope winds (white arrows) and continuation of downvalley winds (blue arrows) from the previous night. The valley is colder than the plain. (b) Mid-morning (approximately 0900 LST): strong slope winds, transition from downvalley to upvalley wind. The valley is the same temperature as the plain. (c) Noon and early afternoon: diminishing slope winds; fully developed upvalley wind. The valley is warmer than the plain. (d) Late afternoon: slope winds have ceased, the upvalley wind continues. The valley is still warmer than the plain. (e) Evening: onset of downslope winds, diminishing upvalley wind. The valley is slightly warmer than the plain. (f) Early night: well developed downslope winds, transition from upvalley wind to downvalley wind. The valley and plain are at same temperature. (g) Middle of the night: downslope winds continue, the downvalley wind is fully developed. The valley is colder than the plain. (h) Late night to morning: downslope winds have ceased and the downvalley wind fills the valley. The valley is colder than the plain.

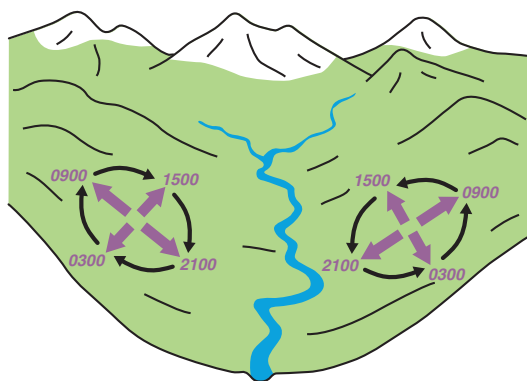


**Figure 11.11** Winds on the left (right) side of a valley turn clockwise (counterclockwise) over the course of a day owing to the combined effects of slope and valley winds. Times are local standard time. (Adapted from Whiteman [1990], whose figure was adapted from a paper by Hawkes [1947].)

this differential heating can also contribute to the overall thermally forced mountain wind system, although cross-valley winds are usually weaker (typically  $\leq 2 \text{ m s}^{-1}$ ) than slope winds and valley winds. Cross-valley winds blow from the colder valley sidewall toward the warmer valley sidewall at low levels, with a compensating flow in the opposite direction at higher altitudes within the valley. The exact magnitude of the cross-valley wind depends on the valley width and cross-valley temperature gradient; the strength of the flow increases with decreasing valley width and increasing temperature differences between the valley sidewalls.

## Further reading

- Banta, R. M., 1990: The role of mountains in making clouds. *Atmospheric Processes over Complex Terrain, Meteor. Monogr.*, No. 45, 229–283.
- Defant, F., 1951: Local winds. *Compendium of Meteorology*, T. M. Malone, Ed. Amer. Meteor. Soc., 655–672.
- de Wekker, S. F. J., S. Zhong, J. D. Fast, and C. D. Whiteman, 1998: A numerical study of the thermally driven plain-to-basin wind over idealized basin topographies. *J. Appl. Meteor.*, **37**, 606–622.
- Egger, J., 1990: Observations of thermally developed wind systems in mountainous terrain. *Atmospheric Processes over Complex Terrain, Meteor. Monogr.*, No. 45, 43–58.
- Haiden, T., 2003: On the pressure field in the slope wind layer. *J. Atmos. Sci.*, **60**, 1632–1635.
- Horst, T. W., and J. C. Doran, 1986: Nocturnal drainage flow on simple slopes. *Bound.-Layer Meteor.*, **34**, 263–286.
- Mahrt, L., 1982: Momentum balance of gravity flows. *J. Atmos. Sci.*, **39**, 2701–2711.
- McKee, T. B., and R. D. O’Neal, 1989: The role of valley geometry and energy budget in the formation of nocturnal valley winds. *J. Appl. Meteor.*, **28**, 445–456.
- Nickus, U., and I. Vergeiner, 1984: The thermal structure of the Inn Valley atmosphere. *Arch. Meteor. Geophys. Bioklim.*, **A33**, 199–215.
- Orville, H. D., 1964: On mountain upslope winds. *J. Atmos. Sci.*, **21**, 622–633.
- Rampanelli, G., D. Zardi, and R. Rotunno, 2004: Mechanisms of up-valley winds. *Mon. Wea. Rev.*, **61**, 3097–3111.
- Steinacker, R., 1984: Area–height distribution of a valley and its relation to the valley wind. *Contrib. Atmos. Phys.*, **57**, 64–71.
- Whiteman, C. D., 1990: Observations of thermally developed wind systems in mountainous terrain. *Atmospheric Processes over Complex Terrain, Meteor. Monogr.*, No. 45, 5–42.
- Whiteman, C. D., 2000: *Mountain Meteorology: Fundamentals and Applications*. Oxford University Press.